Fully Differential Molecular-Frame Measurements for the Electron-Impact Dissociative Ionization of H_2

S. Bellm,[1] J. Lower,[1] E. Weigold,[1] and D. W. Mueller[2]

[1]*AMPL, Research School of Physics and Engineering, Australian National University, Canberra, ACT 0200, Australia*

[2]*Department of Physics, University of North Texas, Denton, Texas, 76203, USA*

(Received 29 October 2009; published 12 January 2010)

We present fully differential state-resolved experimental data for the dissociative ionization of molecular hydrogen induced through electron impact. Molecular-frame ionization cross sections are derived for transitions from the $X^1\Sigma_g^+$ molecular ground state to the $1s\sigma_g$, $2p\sigma_u$, $2s\sigma_g$, and $2p\pi_u$ states of H_2^+. For transitions to the $2s\sigma_g$ and $2p\pi_u$ states, a strong orientation dependence in the cross sections is revealed, with ''side-on'' preferred to ''end-on'' collisions and a propensity for the fragment proton to emerge along the normal to the scattering plane.

DOI: 10.1103/PhysRevLett.104.023202 PACS numbers: 34.80.Dp, 34.80.Pa

The fragmentation of molecular species lies at the heart of many chemical reactions. An important class of molecular fragmentation reactions is the dissociative ionization of molecules induced by charged particle impact. Such reactions play a central role in many atmospheric, industrial, and environmental processes [1–3]. To gain improved insight into their underlying reaction mechanisms, we have performed a kinematically complete study of the dissociative ionization of the simplest molecular species, molecular hydrogen, induced through electron impact.

Recently [4,5], there has been significant theoretical interest in describing molecular-orientation effects for the nondissociative ionization of N_2, CO_2, and H_2 by electron impact. The fully differential scattering cross sections calculated in those studies show a strong dependence on molecular orientation. However, no orientation-resolved experimental data are available to test the predictions. Here, we address the process of dissociative ionization which allows orientation-resolved data to be extracted directly from measurement.

The present study exhibits some similarities to recent photoionization studies of H_2 [6], photo-double-ionization studies of D_2 [7,8], and pump-probe studies involving higher harmonic generation (e.g., [9,10]). In particular [6–8] show that the angular distribution of electrons depends on their emission angle with respect to both light polarization direction and to the molecular axis. However, the interaction of photons with matter, especially for the case of high field strengths, exhibits notable differences to that of charged particles with matter as different angular momentum and symmetry selection rules apply. The present study is pertinent to most cases of dissociative ionization occurring in nature and in industrial processes which are not laser assisted.

Specifically, we consider the reaction

$$e_0^-(\mathbf{p_0}) + H_2 \rightarrow H(n, \mathbf{p_H}) + H^+(\mathbf{p_i}) + e_1^-(\mathbf{p_1}) + e_2^-(\mathbf{p_2}). \quad (1)$$

Here, $e_0^-(\mathbf{p_0})$, $e_1^-(\mathbf{p_1})$, and $e_2^-(\mathbf{p_2})$ represent incident and scattered electrons of respective momenta $\mathbf{p_0}$, $\mathbf{p_1}$, and $\mathbf{p_2}$ (energies E_0, E_1, and E_2). $H(n, \mathbf{p_H})$ represents a hydrogen atom in the electronic state of principle quantum number n, and $\mathbf{p_H}$ is its momentum. $H^+(\mathbf{p_i})$ represents a proton of momentum $\mathbf{p_i}$ (energy E_i).

Given the large mass difference between electrons and protons, post-collision energy-transfer between the hydrogen atom or ion and the continuum electrons is minimal. Thus, $\mathbf{p_i} \cong -\mathbf{p_H}$ and for a known value of $\mathbf{p_0}$, determination of $\mathbf{p_1}$, $\mathbf{p_2}$, and $\mathbf{p_i}$, as achieved in the present triple-coincidence measurement, completely determines the reaction kinematics. Furthermore, by invoking energy conservation, the appearance energy $A(n)$ for transitions to the quantum state n of the residual hydrogen atom is determined through the relation

$$A(n) = \varepsilon_b - 2E_i. \quad (2)$$

Here, ε_b is the electron binding energy, defined by the expression $\varepsilon_b = E_0 - E_1 - E_2$, and $2E_i$ accounts for the kinetic energy shared between the proton and the hydrogen atom. This expression allows ionization events to be sorted according to the dissociation limits of the respective transitions with which they are associated. Finally, assuming the validity of the axial-recoil approximation [11] (which says that fragments resulting from transitions to dissociating molecular states which are short-lived compared with the rotational frequency follow trajectories parallel to the internuclear axis), determination of $\mathbf{p_i}$ enables the molecular orientation at the time of ionization to be inferred and quantities to be determined within the molecular frame.

To date, only few data have been reported for fully differential electron-impact molecular-frame ionization measurements on molecular hydrogen [12–15]. To facilitate discussion, Fig. 1 shows the potential energy diagram for the electronic ground state of H_2 and the four dissociative states of H_2^+ considered in the present and previous studies. In their ground-breaking work, Takahashi *et al.*

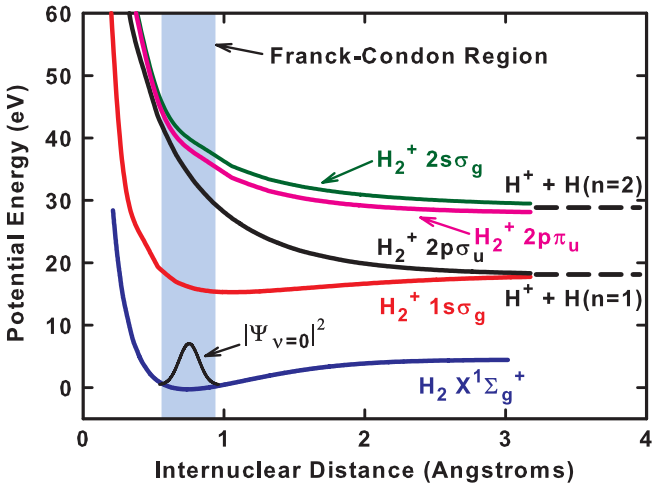

FIG. 1 (color online). Potential energy of H_2 and H_2^+ from [18] as a function of internuclear distance, for the electronic states relevant to the present study. The present measurement resolves transitions to the $2s\sigma_g$ and $2p\pi_u$ states from those to the $1s\sigma_g$ and $2p\sigma_u$ states due to the 10.2 eV separation between their respective dissociation limits as indicated by the dashed lines.

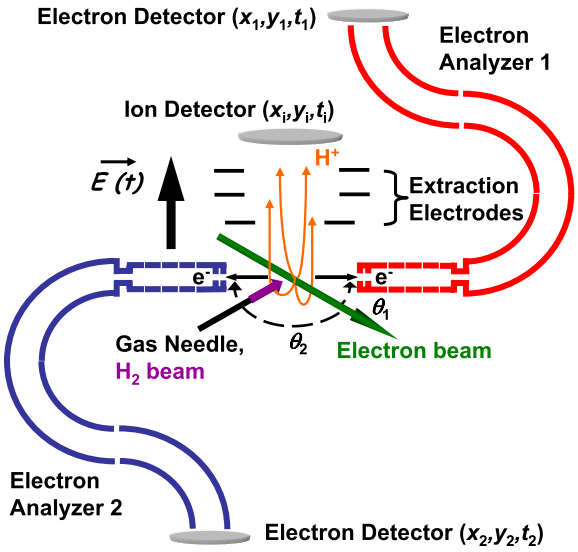

FIG. 2 (color online). Schematic of the triple-coincidence electron–ion spectrometer employed for the present study. See text for details.

[12–14] reported molecular-frame $(e, 2e)$ cross sections for transitions from the electronic ground state $X^1\Sigma_g^+$ to the $2s\sigma_g$ and $2p\sigma_u$ molecular ion states. Measuring only "side-on" collisions of the projectile electron with the molecule, their results showed a transition specific anisotropy in the molecular-frame $(e, 2e)$ cross sections. In contrast, we have developed a spectrometer which measures data for all impact angles of the projectile electron with the molecular-hydrogen target. The improved $(e, 2e)$ binding energy resolution we achieve (2 eV, relative to 7 eV in [12,13]), enabled us to completely resolve transitions to the $2s\sigma_g$ and $2p\pi_u$ states from those to the $1s\sigma_g$ and $2p\sigma_u$ molecular ion states, providing an enhanced level of state selectivity.

Figure 2 shows a schematic of the apparatus (see [16]). Light from an 850 nm laser diode is intercepted by a fast acousto-optical shutter, driven at a frequency of 125 kHz by a pulse generator, to produce a train of 2-microsecond-duration photon pulses. These are focussed onto a gallium arsenide photocathode which, in concert with extraction electrodes, generates an electron beam of identical temporal characteristics. The electron beam is transported at high energy to the collision chamber. There, it is focussed and decelerated to the experimental collision energy E_0 of 178 eV and crosses, at right angles, the molecular-hydrogen target beam formed by effusion through a 0.5 mm bore needle. The intersection of the electron and the hydrogen beam defines a localized interaction volume.

Electrons, emitted within a plane containing the primary-electron beam, are analyzed in one of two toroidal-sector electrostatic momentum analyzers. Analyzer 1 transmits electrons of energy E_1 in the energy range $90\ \text{eV} \leq E_1 \leq 110\ \text{eV}$ over the angular range $10° \leq \theta_1 \leq 50°$ on one side of the electron beam. Analyzer 2 measures electrons of energy E_2 in the energy range $30\ \text{eV} \leq E_2 \leq 50\ \text{eV}$ over the range $30° \leq \theta_2 \leq 70°$ on the other side of the electron beam (see Fig. 2). Energies are determined to $\sim$1 eV and angles to $\sim 2°$, respectively, within the energy and angular acceptance ranges.

Each analyzer incorporates a pair of microchannel-plate electron multipliers followed by a crossed delay-line detector which determines, both spatially and temporally, electron arrival coordinates [17]. Scattered electrons derived from common $(e, 2e)$ ionization events are identified by their correlated arrival times at the two detectors. The momenta of electrons comprising each $(e, 2e)$ pair, $\mathbf{p_1}$ and $\mathbf{p_2}$, respectively, are deduced from their detector arrival coordinates (x_1, y_1, t_1) and (x_2, y_2, t_2), respectively.

Protons, produced by dissociative ionization and emitted over 4π steradians are focussed on to a third delay-line detector by a pulsed electric field. This field $\vec{E}(\mathbf{r}, t)$ results from the application of a fast (several nanoseconds rise time) high voltage pulse to the extraction electrodes surrounding the interaction volume. From the measured proton arrival coordinates (x_i, y_i, t_i) and knowledge of the spatial and temporal characteristics of the extraction field, the proton momentum $\mathbf{p_i}$ is deduced.

Employing the same pulse generator output used to produce the pulsed electron beam, the needle potential is modulated between voltage levels of 0 and 180 V to enable, respectively, measurement and cleaning cycles to be performed. The cleaning cycle prevents the buildup of low-energy ions which might otherwise lead to background events.

At the start of the measurement cycle, the extraction electrodes and the needle are set to ground potential, and an electron pulse of 2 microseconds duration is fired into

the interaction volume. A coincidence unit, monitoring pulses from the two electron detectors, detects coincident electron arrivals. If no $(e, 2e)$ event is measured within the measurement cycle, the extraction electrodes and needle remain at zero potential throughout its duration. If an $(e, 2e)$ electron pair is detected (a) the extraction field is turned on for a duration of 10 microseconds, a sufficient time for the associated H^+ or H_2^+ ion to travel to the ion detector and (b) the needle voltage is raised to 180 V, the appropriate value of potential to avoid disturbing the extraction field, for the same duration. Because of the factor of 2 difference in mass between H^+ and H_2^+ ions, their respective arrival times at the ion detector are sufficiently well separated to completely resolve dissociative from nondissociative ionization events.

In the cleaning cycle, the extraction electrodes are grounded, and the needle potential is raised to 180 V. This action expels any ion(s) created in the previous measurement cycle but not extracted. An extremely low level of primary-electron beam current (~35 pA) was employed to ensure that the probability that measured triple coincidences, comprising electrons and ions derived from different ionization events, remained extremely low (~10% of total triple-coincidence signal). Details of the employed background subtraction procedure will be described in a future publication.

Figure 3 shows the adopted reaction kinematics. A relatively low value of 178 eV was chosen for the incident electron energy to increase the proportion of ionization events leading to dissociation. The mean energy value for the slow scattered electrons (40 eV) was chosen as a compromise between maximizing ionization count rates (lower values for E_2) and minimizing the effects of chromic aberration in the analyzer imaging system (higher E_2 values).

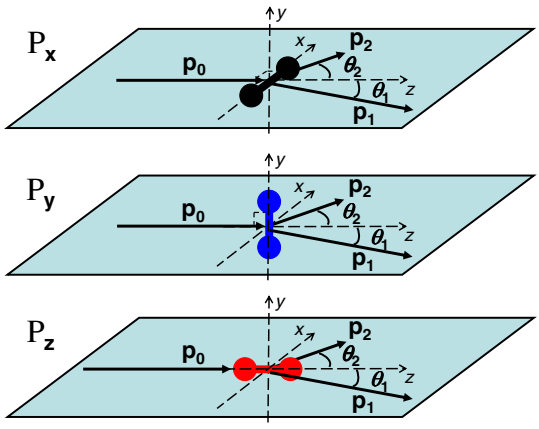

FIG. 3 (color online). Experimental reaction kinematics. Electrons of momentum $\mathbf{p_0}$, traveling along the z axis, ionize an unoriented ensemble of hydrogen molecules. Scattered electrons, emitted in the x-z plane and of respective momenta $\mathbf{p_1}$ and $\mathbf{p_2}$, are detected. For molecules which undergo dissociative ionization, their orientation at the time of ionization is deduced from the momentum $\mathbf{p_i}$ of the released proton. The figure shows collisions involving the three orthogonal molecular orientations $\mathbf{P_x}$, $\mathbf{P_y}$, and $\mathbf{P_z}$. The projectile-electron energy E_0 is 178 eV, and the average energies E_1 and E_2 of the two measured scattered electrons are 100 and 40 eV, respectively.

Figure 4 shows experimental results for the dissociative ionization process described by Eq. (1). Triple-coincidence counts are displayed as a function of proton energy E_i and the electron binding energy ε_b. Regions of high intensity, associated with different transitions, are highlighted. Transitions to the $1s\sigma_g$ and $2p\sigma_u$ states are completely resolved as their proton energy distributions are energetically separated from one another and their dissociation limit is separated by 10.2 eV from that for transitions to the $2s\sigma_g$ and $2p\pi_u$ states. Transitions to the latter two states, however, cannot be resolved from one another as their proton energy distributions overlap, and they share identical dissociation limits.

Figure 5 shows the triple-coincidence count rates for combined transitions to the $2s\sigma_g$ and $2p\pi_u$ states of H_2^+ as a function of the fast-electron scattering-angle θ_1. The data have been averaged over the slow-electron scattering angle θ_2 to improve statistics. Results are displayed for the three molecular orientations $\mathbf{P_x}$, $\mathbf{P_y}$, and $\mathbf{P_z}$ as defined in Fig. 3. Data for these orientations was obtained by selecting only those triple-coincidence events corresponding, respectively, to ion momenta $\mathbf{p_i}$ aligned to within 10 degrees of each of the three coordinate axes.

Comparing the data for the three orientations, most striking is the propensity of the proton to be emitted along the normal to the scattering plane, defined by the momenta

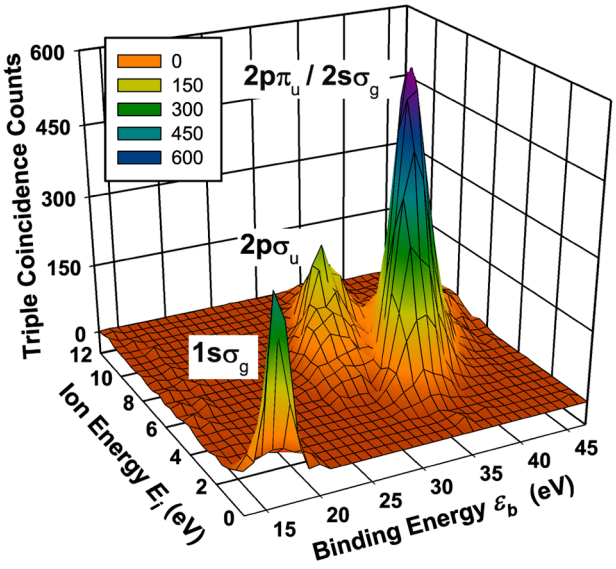

FIG. 4 (color online). Triple-coincidence counts as a function of proton energy E_i and electron binding energy ε_b. Maxima in the ion energy distributions are associated with transitions to the ground and to the first excited state of the residual hydrogen atom as indicated.

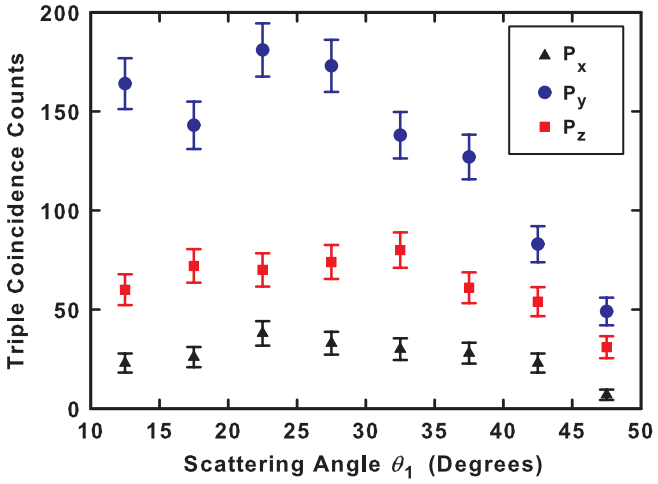

FIG. 5 (color online). Triple-coincidence counts for transitions to the $2s\sigma_g$ and $2p\pi_u$ states of H_2^+ as a function of the fast-electron scattering angle θ_1 for the three molecular orientations $\mathbf{P_x}$, $\mathbf{P_y}$, and $\mathbf{P_z}$. Kinematics as in Fig. 3. The data have been averaged over the slow-electron scattering angle θ_2.

of the incoming and measured scattered electrons. In other words, dissociative ionization favors a "side-on" collision with the molecular axis perpendicular to the scattering plane ($\mathbf{P_y}$ orientation). Indications of such an effect for transitions to the $2p\sigma_u$ state were seen in the data of Takahashi *et al.* [14] under different reaction kinematics. A strong effect is confirmed in the present case. "Side-on" collisions corresponding to the ejection of a proton within the scattering plane ($\mathbf{P_x}$ orientation) are the least favored. "End-on" collisions ($\mathbf{P_z}$ orientation) fall between these two extremes. The number of accumulated triple-coincidence counts is seen to vary with the fast-electron scattering angle θ_1, and hence the momentum transfer from the projectile to the target molecule. However, the ordering in the relative preference for ionization to favor each of the three orientations does not. Given the complexity of the dissociative ionization problem, a detailed theoretical analysis will be required to establish whether the present findings are amenable to simple physical interpretation.

In conclusion, we have presented fully differential results for the dissociative ionization of molecular hydrogen induced by electron impact. By invoking the axial-recoil approximation, our results show a strong dependence of the dissociation rate on the orientation of the molecular axis with respect to both the momentum vector of the projectile electron and to the normal to the scattering plane. For combined transitions to the $2s\sigma_g$ and $2p\pi_u$ states, dissociative ionization is found to favor molecular orientations normal to the scattering plane for all measured values of momentum transfer. A detailed analysis of the results will appear in a future publication. The work suggests that molecular orientation could be used as an additional variable to optimize chemical reactions driven by directed beams of charged particles.

We gratefully acknowledge the assistance of the Australian Research Council under Grants No. DP0452553 (S. B., J. L., and E. W.) and No. DP0663587 (S. B.). D. W. M. gratefully acknowledges support from the Centre for Antimatter-Matter Studies during his visit to ANU.

[1] V. I. Shematovich, R. E. Johnson, M. Michael, and J. G. Luhmann, J. Geophys. Res. **108**, 5087 (2003).
[2] J. Liu, F. Sun, and H. Yu, Current Applied Physics 6, (2005) 625.
[3] I. IPolyi, P. Cicman, S. Denifl, V. Matejčík, P. Mach, J. Urban, P. Scheier, T. D. Märk, and Š. Matejčík, Int. J. Mass Spectrom. **252**, 228 (2006).
[4] O. Al-Hagan, C. Kaiser, D. Madison, and A. J. Murray, Nature Phys. **5**, 59 (2009).
[5] J. Colgan, M. S. Pindzola, F. Robicheaux, C. Kaiser, A. J. Murray, and D. H. Madison, Phys. Rev. Lett. **101**, 233201 (2008).
[6] Y. Hikosaka and J. H. E. Eland, Chem. Phys. **277**, 53 (2002).
[7] Th. Weber, A. Czasch, O. Jagutzki, A. Müller, V. Mergel, A. Kheifets, J. Feagin, E. Rotenberg, G. Meigs, M. H. Prior, S. Daveau, A. L. Landers, C. L. Cocke, T. Osipov, H. Schmidt-Böcking, and R. Dörner, Phys. Rev. Lett. **92**, 163001 (2004).
[8] Th. Weber, A. Czasch, O. Jagutzki, A. K. Müller, V. Mergel, A. Kheifets, E. Rotenberg, G. Meigs, M. H. Prior, S. Daveau, A. Landers, C. L. Cocke, T. Osipov, R. Díez Mulño, H. Schmidt-Böcking, and R. Dörner, Nature (London) **431**, 437 (2004).
[9] Anh-Thu Le, R. R. Lucchese, M. T. Lee, and C. D. Lin, Phys. Rev. Lett. **102**, 203001 (2009).
[10] T. Kanai, S. Minemoto, and H. Sakai, Nature (London) **435**, 470 (2005).
[11] R. N. Zare, Mol. Photochem. **4**, 1 (1972).
[12] M. Takahashi, N. Watanabe, Y. Khajuria, K. Nakayama, Y. Udagawa, and J. H. D. Eland, J. Electron Spectrosc. Relat. Phenom. **141**, 83 (2004).
[13] M. Takahashi, N. Watanabe, Y. Khajuria, Y. Udagawa, and J. H. D. Eland, Phys. Rev. Lett. **94**, 213202 (2005).
[14] M. Takahashi, Bull. Chem. Soc. Jpn. **82**, 751 (2009).
[15] A. Dorn, Bull. Am. Phys. Soc. **51**, 78 (2006).
[16] J. Lower, R. Panajotovic, S. Bellm, and E. Weigold, Rev. Sci. Instrum. **78**, 111301 (2007).
[17] R. Dörner, V. Mergel, O. Jagutzki, L. Spielberger, J. Ullrich, R. Moshammer, and H. Schmidt-Böcking, Phys. Rep. **330**, 95 (2000).
[18] T. E. Sharp, Atomic Data **2**, 119 (1971).